Journal of Molecular Liquids 213 (2016) 107–114

Contents lists available at ScienceDirect

Journal of Molecular Liquids

journal homepage: www.elsevier.com/locate/molliq

Solvatochromic parameters of imidazolium-, hydroxyammonium-, pyridinium- and phosphonium-based room temperature ionic liquids

Juan M. Padró, Mario Reta *

Laboratorio de Investigación y Desarrollo de Métodos Analíticos (LIDMA), División Química Analítica, Facultad de Ciencias Exactas, (UNLP), 47 y 115, (1900) La Plata, Buenos Aires, Argentina

ARTICLE INFO

Article history:
Received 17 September 2015
Accepted 4 October 2015
Available online xxxx

Keywords:
Room temperature ionic liquids
Solvatochromic solvent parameters
Nitrogen-based ionic liquids
Phosphonium-based ionic liquids
Partition coefficients

ABSTRACT

Solvatochromic solvent parameters of different room temperature ionic liquids based on the imidazolium, hydroxyammonium, pyridinium and phosphonium cations, namely 1-butyl-3-methyl imidazolium hexafluorophosphate, 1-hexyl-3-methyl imidazolium hexafluorophosphate, 1-octyl-3-methyl imidazolium hexafluorophosphate, 1-octyl-3-methyl imidazolium tetrafluoroborate, *N*-octylpyridinium tetrafluoroborate, 2-hydroxyethylammonium formate, 2-hydroxypropylammonium formate, trihexyl-(tetradecyl)phosphonium chloride, trihexyl-(tetradecyl)phosphonium bromide, trihexyl-(tetradecyl)phosphonium bis(trifluoromethylsulfonyl)imide and trihexyl-(tetradecyl)phosphonium dicyanamide were determined at 25 °C using UV–Vis spectroscopy. Specifically, we have measured the Kamlet–Taft parameters: α (hydrogen-bond donor acidity), β (hydrogen-bond acceptor basicity), π^* (dipolarity/polarizability) and the Reichardt's normalized polarity parameter, E_T^N.

In previous works, we employed the Solvation Parameter Model to predict the partition coefficients for compounds of biological and pharmacological interest and to elucidate the chemical interactions involved in the partition process of different probe molecules between water and different types of ionic liquids. In this work, we have used the obtained solvatochromic solvent parameters to explain and understand the relative magnitudes of the chemical interactions obtained with the solvation parameter model.

1. Introduction

In the past decades, ionic liquids have been increasingly used for diverse applications such as organic synthesis [1,2], catalysis [3,4], electrochemical devices [5,6], and solvent extraction of a variety of compounds in addition to many other areas [7–10]. At present, room temperature ionic liquids (RTILs) are close to be considered as conventional solvents for extraction and sample preparation, although their use compared with typical organic solvents is still much lower [8]. The use of ionic liquids in different areas of Analytical Chemistry, particularly the RTILs, has increased considerably in recent years [8,11–13]. This is because these solvents have several characteristics that are different to those of the typical organic solvents, such as unique solubilization properties, low or none vapor pressure, no flammability and the possibility to modify their physical properties through the proper selection of the cation and anion [14,15].

Ionic liquids offer a great flexibility in their properties since the possible combinations of cations and anions are quite high. However, a wide variety of cations and anions available make a systematic study of their physicochemical properties very difficult. The selection of an appropriate ionic liquid for a particular application would require a comprehensive database of the fundamental properties like stability, density, miscibility, viscosity, and polarity for a wide range of temperature and pressure, which unfortunately at present is not available for all the classes of ionic liquids. The polarity of ionic liquids can play a crucial role in optimizing the reaction conditions for organic transformation in addition to other vital applications. For example, the high polarity of the cation pyrrolidinium, a Brønsted acid, was considered to be an important factor for the oxidative desulfurization of diesel fuel in the presence of H_2O_2 [16].

The polarity of several ionic liquids has been studied in terms of the Reichardt's normalized scale, E_T^N [17–19] and the Kamlet–Taft polarity parameter, π^*, for several ionic liquids [19–22]. Recent publications have shown that the commonly used ionic liquids are reasonably polar solvents, having polarity greater than those of solvents like acetone and dimethyl sulfoxide but less than water and short-chain alcohols [21,23,24]. A comprehensive account of the polarity of ionic liquids has been presented by C. Reichardt [17].

The ionic liquids properties have revealed many interesting characteristics not observed earlier for conventional solvents. For example, ionic liquids show a strong tendency of preferential solvation for a probe molecule in their binary mixtures with water or organic cosolvents. Although preferential solvation has been observed also in conventional binary mixtures, the effect was not as drastic as was seen in ionic liquid mixtures. The polarity studies on the binary mixture of

* Corresponding author.
E-mail address: mreta@quimica.unlp.edu.ar (M. Reta).

http://dx.doi.org/10.1016/j.molliq.2015.10.055
0167-7322/

tetraethylene glycol with the ionic liquid 1-butyl-3-methylimidazolium hexafluorophosphate, [BMIM][PF_6], showed interesting synergistic effects, which was termed as "hyperpolarity" [25]. It is believed that such phenomena arise due to the formation of highly ordered microsegregated phases in the binary mixtures.

Although phosphonium-based RTILs (PB-RTILs) have been known and synthesized for years, they have been more or less "neglected" in the literature compared to their imidazolium or pyrrolidinium based counterparts [26]. PB-RTILs are made of tetra-alkyl-phosphonium cations with different anions and can have some additional advantages compared to the nitrogen-based RTILs (NB-RTILs), such as very high thermal and chemical stability and higher solvation properties. There are about 20 different types of PB-RTILs commercially available. Cytec Industries Inc. sells phosphonium salts under the CYPHOS® trade name [27,28]. PB-RTILs have much low cost as compared to NB-RTILs and some of them have lower density than water, and advantage in extraction processes.

In previous works [26,28], we have used the Solvation Parameter Model (SPM) to elucidate the molecular interactions involved in the partition process for analytes of very different chemical nature between NB- and PB-RTILs and water. Also, we could predict liquid–liquid partition coefficients for molecules of biological and pharmacological interest. This finding will allow to theoretically predict which RTIL will be useful to obtain high recoveries and enrichment factors for any analyte (neutral at the working pH) when this type of new solvents are used as extractant.

The SPM relates the logarithm of some free-energy related physicochemical property, in this case the RTIL-water partition coefficient, $P_{IL/w}$, and several independent solute parameters or descriptors, each one reflecting a different type of solute–solvent interaction (Eq. 1). Thus, since a solvation process (relative solubility of the analyte in a biphasic system) is involved, the SPM is considered as linear solvation energy relationship (LSER).

$$\log P_{IL/w} = \mathbf{c} + \mathbf{s}S + \mathbf{aA} + \mathbf{bB} + \mathbf{vV} + \mathbf{eE} \quad (1)$$

Here the solute descriptors are as follows: **S** is the solute dipolarity/polarizability; **A** and **B** are the respective solute hydrogen-bond acidity and basicity; **V**, the molar volume, accounts for both cohesive interactions (the necessary energy to form the cavity within the solvent to fit the solute) and dispersive interactions, and **E**, the excess molar refraction, accounts for interactions with electron-donor groups. The intercept, **c**, and the regression coefficients **s**, **a**, **b**, **v**, and **e** (LSER coefficients) are obtained from multivariable, simultaneous, least-squares regressions [29]. These coefficients contain chemical information since they reflect the *difference between the RTIL phase and the aqueous phase* in the complementary property to each solute parameter [29–32] as follows:

$$\log P_{IL/w} = c + s'(\mathbf{s_{IL}}-\mathbf{s_w})\mathbf{S} + a'(\mathbf{b_{IL}}-\mathbf{b_w})\mathbf{A} + b'(\mathbf{a_{IL}}-\mathbf{a_w})\mathbf{B} + v'(\mathbf{v_{IL}}-\mathbf{v_w})\mathbf{V} + e'(\mathbf{e_{IL}}-\mathbf{e_w})\mathbf{E} \quad (2)$$

where the subscripts "IL" and "w" denote the water-saturated ionic liquid phase and the ionic liquid-saturated water phase, respectively. The coefficients s′, a′, b′, v′ and e′ are fitting parameters which ought to be independent of the solute and liquid phases if the formalism were rigorously correct [33,34]. The nomenclature was adapted from reference [29] to this work. It was suggested that the $v'(\mathbf{v_{IL}}-\mathbf{v_w})\mathbf{V}$ term can be dissected into a "cavity term" and a "dispersive term" [26,29].

$$v'(\mathbf{v_{IL}}-\mathbf{v_w})\mathbf{V} = v'_1(\boldsymbol{\sigma}_{IL}-\boldsymbol{\sigma}_w)\mathbf{V} + v'_2(\mathbf{D_{IL}}-\mathbf{D_w})\mathbf{V} \quad (3)$$

Here $\boldsymbol{\sigma}$ denotes some measure of the cohesive energy density of forming a "hole" in a solvent and **D** is a dispersion parameter representing the strength or susceptibility of the solvent to engage in London interactions. Based on the solubility parameter theory, $\boldsymbol{\sigma}$ can be taken as the square of Hildebrand solubility parameter, δ_H^2 [29]. Unfortunately, dispersion parameters representing the **D** term are not available in the literature for any liquid and δ_H values are known for a few RTILs [35,36].

In this work, we have obtained the solvatochromic solvent parameters π^* of polarity–polarizability, β of hydrogen bond acceptor capacity and α of hydrogen bond donor capacity for imidazolium-, pyridinium-, hydroxyammonium- and phosphonium-based ionic liquids. For validation purpose, we obtained these parameters for some RTILs already reported in the literature. The α parameter was obtained indirectly through the Reichardt's normalized solvent parameter, E_T^N. The obtained solvent parameters were used to understand and explain the chemical interactions involved in biphasic systems formed by different ionic liquids and water studied in previous works.

2. Experimental

2.1. Chemicals and materials

Trihexyl-(tetradecyl)phosphonium chloride, [$(C_6)_3C_{14}P$][Cl] (CYPHOS® IL 101), trihexyl-(tetradecyl)phosphonium bromide, [$(C_6)_3C_{14}P$][Br] (CYPHOS® IL 102), trihexyl-(tetradecyl)phosphonium dicyanamide, [$(C_6)_3C_{14}P$][$N(CN)_2$] (CYPHOS® IL 105) and trihexyl-(tetradecyl)phosphonium bis(trifluoromethylsulfonyl)imide, [$(C_6)_3C_{14}P$][NTf_2] (CYPHOS® IL 109) were provided by Cytec Industries Inc. (New Jersey, USA). 1-hexyl-3-methylimidazolium hexafluorphosphate [HMIM][PF_6], 97.0% (Fluka Buchs, Germany). *N*-octylpyridinium tetrafluoroborate, [OPy][BF_4] was synthesized and purified in our laboratory by adapting a procedure from Ref. [37]. 1-octyl-3-methylimidazolium hexafluorophosphate, [OMIM][PF_6], 1-butyl-3-methylimidazolium hexafluorophosphate [BMIM][PF_6] and 1-octyl-3-methylimidazolium tetrafluoroborate [OMIM][BF_4] were synthesized and purified in our laboratory by adapting a procedure from Ref. [26,28]. 2-Hydroxypropylammonium formate [OH–C_3NH_3][For] and 2-Hydroxyethylammonium formate [OH–C_2NH_3][For] were obtained and purified as previously reported in by adapting a procedure from Ref. [38]. In Fig. 1, the chemical structures for these studied RTILs are shown. In Table 1, the names and the corresponding abbreviations are depicted.

Reagents were of analytical grade or better: sodium hexafluorophosphate, 98.0% (Aldrich, Wisconsin, USA), *1*-Methylimidazole, ≥99.0% (Merck, Hohenbrunn, Germany), 2-aminoethanol (Fluka, Buchs, Switzerland), pyridine, 99.0% (Sigma-Aldrich, St. Louis, USA), tetrafluoroboric acid, 48.0% (w/v) in water (Sigma-Aldrich, St. Louis, USA), *N*,*N*-diethyl-*4*-nitroaniline (Frinton Laboratories Inc., NJ, USA), *4*-nitroaniline and Reichardt's dye 30 (Sigma-Aldrich, St. Louis, USA), sodium hydroxide and potassium hydroxide (Analar, Poole, England), *1*-Bromoctane, 99.0% (Aldrich, WI, USA), sodium sulfate anhydrous (Merck, Buenos Aires, Argentina), silver nitrate and formic acid 85.0% (Anedra, Industria Argentina), acetonitrile (Carlo Erba, Divisione Chimica Industriale—Milano, Italy), acetone (Merck, Industria Argentina), ethanol anhydrous (Carlo Erba, Divisione Chimica Industriale—Milano, Italy) and methanol and dichloromethane HPLC grade (J. T. Baker, Edo. de Mexico, Mexico). The micropipettes were purchased from Eppendorf, Hamburg, Germany.

2.2. Equipment

A single-beam Helios-Gamma UV–Vis spectrophotometer (Thermo) with 1 mm path length quartz cuvettes was used to register the UV–Vis spectra for the different probe molecules shown in Fig. 2 used to obtain the solvent parameters. A thermostat controlled bath (Lauda T) maintained at 25.00 ± 0.05 °C was employed for the experiments, a Vortex Genie 2 (Scientific Industries, USA) mixer allowed thorough mixture of the aqueous and the RTIL phases. Water was purified with a Milli-Q system (Millipore Co.).

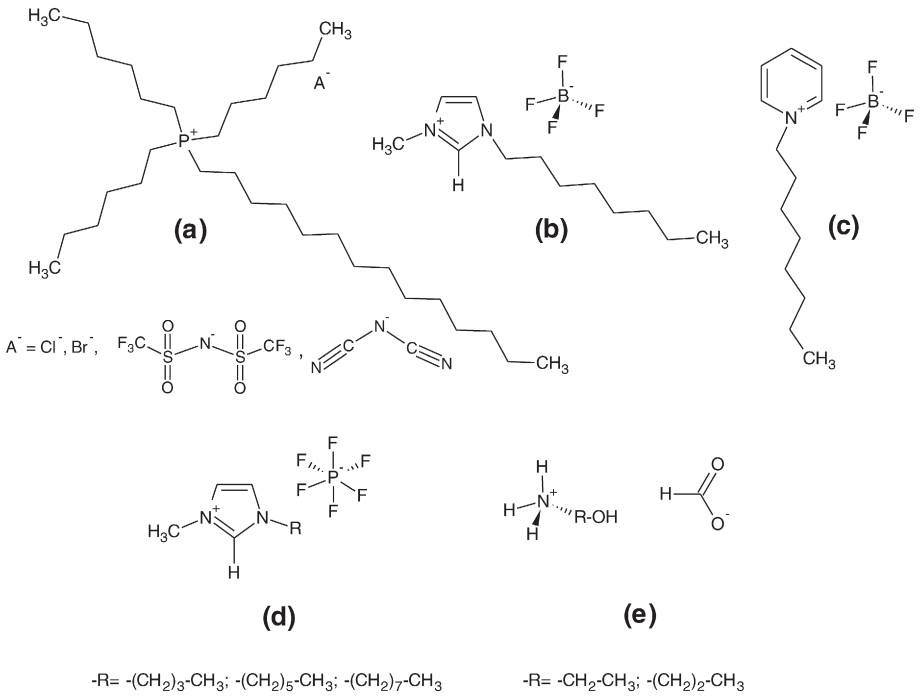

Fig. 1. Room temperature ionic liquids used to obtain the solvatochromic solvent parameters. Phosphonium-based RTILs, (a) $[(C_6)_3C_{14}P][A]$; Nitrogen-based RTILs, (b) $[OMIM][BF_4]$, (c) $[OPy][BF_4]$, (d) $[R–MIM][PF_6]$ and (e) $[OH–RNH_3][For]$.

2.3. Procedure to obtain the solvent parameters

The phosphonium-based RTILs were washed with an alkaline solution as follows: a mixture of the ionic liquid and dichloromethane, DCM (1:4 ratio) was washed with different aliquots of 1 ml, shaked and centrifuged for 10 min at 4200 rpm to separate the two phases. The first five contacts were done with an aqueous solution of KOH 10^{-4} M, and the five final contacts were done with 1 ml MilliQ water to eliminate any rest of the alkaline solution. The absence of the RTIL anions coming from the original reactive was checked by reaction with aqueous solution of $AgNO_3$ 0.01 M. Then, solid anhydrous Na_2SO_4 was added to eliminate traces of water; the mixtures were shaked for 15 min and filtered through a Whatman® 40 filter paper. The DCM layer was then concentrated on a rotary evaporator and dried under vacuum at 50 °C for 48 h. The neat RTILs obtained were then used to measure the solvent parameters. Aliquots of aqueous solutions of the different probe molecules (Fig. 2) selected to obtain the solvent parameters were added to the different RTILs and brought to 25 °C in a thermostatic bath to measure the UV–Vis spectra. The maximum wavelengths of the different absorption bands were used to calculate the Kamlet–Taft π^*, β, α and E_T^N solvent parameters.

Table 1
RTILs employed for the determination of the solvatochromic parameters.

Abbreviations	RTILs' names
$[BMIM][PF_6]$	1-butyl-3-methylimidazolium hexafluorphosphate
$[HMIM][PF_6]$	1-hexyl-3-methylimidazolium hexafluorphosphate
$[OMIM][PF_6]$	1-octyl-3-methylimidazolium hexafluorphosphate
$[OMIM][BF_4]$	1-octyl-3-methylimidazolium tetrafluoroborate
$[OPy][BF_4]$	*N*-octylpyridinium tetrafluoroborate
$[OH–C_2NH_3][For]$	2-Hydroxy ethylammonium formate
$[OH–C_3NH_3][For]$	2-Hydroxy propylammonium formate
$[(C_6)_3C_{14}P][N(CN)_2]$	Trihexyl-(tetradecyl)phosphonium dicyanamide
$[(C_6)_3C_{14}P][NTf_2]$	Trihexyl-(tetradecyl)phosphonium bis(trifluoromethylsulfonyl)imide
$[(C_6)_3C_{14}P][Cl]$	Trihexyl-(tetradecyl)phosphonium chloride
$[(C_6)_3C_{14}P][Br]$	Trihexyl-(tetradecyl)phosphonium bromide

2.3.1. Determination of the E_T^N parameter

0.60 mL of washed ionic liquid was dried under vacuum at 50 °C for 5–8 h. A solution of the Reichardt's dye 30 was prepared in freshly distilled DCM under nitrogen using 0.0025 g of dye in a 5.0 mL volumetric flask. To the pure ionic liquid, 0.50 mL of the dye solution was added (under nitrogen) and the DCM was removed under vacuum. In case the RTIL remained blue or green (depending on the RTIL type) after addition of the dye, it was left under vacuum for 2 h more before measurement. If the solution is colorless, it means that the charge-transfer band disappeared because the oxygen atom of the Reichardt's dye 30 phenolate anion is protonated by the water molecules. In this case, the washing procedure was repeated as many times as necessary to eliminate water traces and to obtain a colored ionic liquid solution. The E_T^{30} solvent parameter was calculated according to Eq. 4 [20,39–41].

$$E_T^{30}/kcal\ mol^{-1} = \frac{28591}{\lambda_{max}/nm} \quad (4)$$

where λ_{max} is the wavelength corresponding to the maximum of the intramolecular charge transfer absorption band of the Reichardt's dye 30.

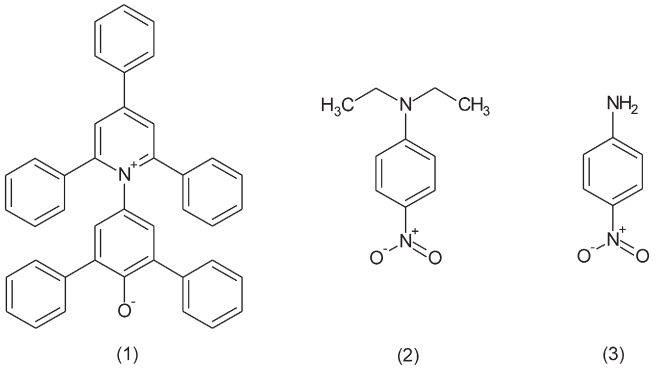

Fig. 2. Reichardt's dye (1), *N*,*N*-diethyl-4-nitroaniline (2), and 4-nitroaniline (3) used as probe molecules to obtain the solvatochromic solvent parameters.

The scale E_T^N is the E_T^{30}scale normalized between the values of 0 (for trimethylsilane, TMS) and 1 (for water). It was calculated according to Eq. 5 [40,42].

$$E_T^N = \frac{E_T^{30}(solv) - E_T^{30}(TMS)}{E_T^{30}(water) - E_T^{30}(TMS)} = \frac{E_T^{30}(solv) - 30.7}{32.4} \quad (5)$$

2.3.2. Determination of the Kamlet–Taft solvent parameters π, β and α*

0.0044 g of *N,N*-diethyl-*4*-nitroaniline for the determination of the π^* parameter or 0.0042 g of *4*-nitroaniline for the determination of the β parameter was dissolved in a 25.0 mL volumetric flask, using DCM. Roughly 0.40 mL of this solution was added to the 0.60 mL ionic liquid sample and the DCM was evaporated under vacuum. Since the RTILs have no vapor pressure, they remain in the flask with the dissolved probe molecules. The π^* parameter was calculated according to Eq. 6 [39,43,44].

$$\pi^* = \frac{(27.52 - \nu_{max})}{3.182} \quad (6)$$

and the β solvent parameter according to Eq. 7 [39,44,45]:

$$\beta = \frac{(31.10 - \nu_{max} - 1.12\pi^*)}{2.79}. \quad (7)$$

Here, $\upsilon_{max} = 1/\lambda_{max}(nm)10^{-4}$; υ_{max} (in kiloKaisers, kK, where $1kK = 1000\ cm^{-1}$) is the wavenumber corresponding to the wavelength of the maximum absorption band, λ_{max}, of the corresponding probe molecule.

The α parameter was determined by using the E_T^N parameter according to Eq. 8 [39,44,45].

$$\alpha = \frac{(10.94 - \nu_{max} - 3.88\pi*)}{5.39} \quad (8)$$

where υ_{max} (in kK) is the wavenumber corresponding to the wavelength of the maximum absorption band, λ_{max}, of the Reichardt dye 30.

3. Results and discussion

3.1. Solvent parameters for neat solvents

Kamlet and Taft have established solvent scales of hydrogen-bond basicity, β, hydrogen-bond acidity, α, and polarity–polarizability, π^*, which account for the interactions taking place in a given solvent. These parameters are known for water, typical organic solvents [45], some NP-RTILs and a few PB-RTILs [11,19,20,46]. In Table 2 we show the π^*, β, α and E_T^N parameters for NP-RTILs and PB-RTILs. Some of these parameters were already obtained in the literature but, in order to validate the experimental procedure and simultaneously check the purity of the used RTIL, we have obtained those solvent parameters again and, also, for three different organic solvents with comparison purposes. As can be observed in Table 2, the solvent parameter values for the NB-RTILs agree very well with the obtained by other authors, which validates the determination procedure and confirms the purity of the RTILs used. Up to our knowledge, there is just one report about Kamlet–Taft solvent parameters for PB-RTILs [20]. The authors used also a tetra-alkyl-phosphonium cation but with very different anions (alanate and valinate) to the ones selected in this study. The average values for the solvent parameters were 0.95 for the polarity–polarizability parameter, π^*, 1.2 for the hydrogen-bond acceptor (HBA) solvent parameter, β, and 0.8 for the hydrogen-bond donor (HBD) solvent parameter, α, respectively. The π^* and β values are in agreement with the ones in Table 2, but very different α values were obtained, which can be attributed to a higher hydrogen-bond donor capacity of the alanate and valinate anions due to the $-NH_3^+$ groups.

Table 2
Solvent parameters of the studied RTILs and some polar solvents. E_T^N: normalized polarity parameter of Dimroth–Reichardt; Solvent parameters of Kamlet–Taft: π^*, polarity–polarizability; α, hydrogen-bond donor, and β, hydrogen-bond acceptor.

	E_T^N	π^*	α	β	δ_H ($MPa^{1/2}$)
[BMIM][PF_6]	0.662 ± 0.004 (0.667[a]; 0.669[h]; 0.667[k])	1.03 ± 0.04 (1.032[a]; 0.90[i]; 1.04[j])	0.64 ± 0.02 (0.634[a]; 0.54[i]; 0.63[j])	0.21 ± 0.02 (0.207[a]; 0.44[i]; 0.19[j])	(28.09; 29.8–30.2[m])
[HMIM][PF_6]	0.654 ± 0.002 (0.66[b])	1.01 ± 0.03 (1.02[b]; 0.93[i])	0.62 ± 0.02 (0.63[b]; 0.51[i])	0.22 ± 0.03 (0.24[b]; 0.50[i])	(28.6[m])
[OMIM][PF_6]	0.628 ± 0.004 (0.633[c]; 0.636[a])	0.87 ± 0.04 (0.88[c]; 0.92[i])	0.58 ± 0.03 (0.58[c]; 0.52[i])	0.45 ± 0.04 (0.46[c]; 0.53[i])	(27.8[m])
[OMIM][BF_4]	0.642 ± 0.004 (0.65[b]; 0.543[a])	0.96 ± 0.03 (0.98[b]; 0.93[i])	0.60 ± 0.03 (0.62[b]; 0.45[i])	0.39 ± 0.04 (0.41[b]; 0.63[i])	(22.5[m])
[OPy][BF_4]	0.604 ± 0.005 (0.606[d])	0.97 ± 0.03 (0.974[d])	0.52 ± 0.05 (0.535[d])	0.33 ± 0.03 (0.340[d])	–
[OH–C_2NH_3][For]	0.91 ± 0.02 (0.89[f]; 0.891[g])	1.14 ± 0.04 (1.15[f])	0.99 ± 0.02 (1.01[f])	0.59 ± 0.04 (0.59[f])	–
[OH–C_3NH_3][For]	0.870 ± 0.004	1.09 ± 0.02	0.98 ± 0.02	0.64 ± 0.05	–
[$(C_6)_3C_{14}P$][$N(CN)_2$]	0.433 ± 0.006	0.93 ± 0.05	0.20 ± 0.03	1.36 ± 0.05	–
[$(C_6)_3C_{14}P$][NTf_2]	0.420 ± 0.003	0.89 ± 0.03	0.20 ± 0.02	1.24 ± 0.04	(18.7[o])
[$(C_6)_3C_{14}P$][Cl]	0.444 ± 0.005	0.87 ± 0.04	0.27 ± 0.03	1.56 ± 0.03	(19.9[o])
[$(C_6)_3C_{14}P$][Br]	0.397 ± 0.007	0.87 ± 0.05	0.17 ± 0.04	1.57 ± 0.05	–
Ethanol	0.657 ± 0.002 (0.654[e])	0.60 ± 0.05 (0.54[e])	0.91 ± 0.06 (0.86[e])	0.75 ± 0.03 (0.75[e])	(26.0[n])
Ethyl acetate	(0.23[e])	(0.55[e])	(0.00[e])	(0.45[e])	(18.6[n])
Acetonitrile	0.478 ± 0.004 (0.459[e])	0.78 ± 0.04 (0.75[e])	0.22 ± 0.04 (0.19[e])	0.37 ± 0.03 (0.40[e])	(24.3[n])
Water	(1.00[e])	(1.09[e])	(1.17[e])	(0.47[e])	(47.9[n])

Data from reference.
[a] [46].
[b] [53].
[c] [1].
[d] [20].
[e] [45].
[f] [54].
[g] [55].
[h] [41].
[i] [56].
[j] [21].
[k] [17].
[m] [35].
[n] [40].
[o] [57].

3.1.1. π^* parameter

As can be observed in Table 2, polarity–polarizability is slightly higher for NB-RTILs than for PB-RTILs which could be attributed to the higher polarizability of the aromatic rings, not present in the PB-RTILs (*c.f.* Fig. 1). These NB-RTILs can be as polar as pure water ($\pi^* = 1.09$) and the obtained values are very close to those published in the literature for other nitrogen-based RTILs [8]. PB-RTILs studied in this paper are less polar than water but more polar than acetonitrile or ethanol (see Table 2).

3.1.2. β parameter

It can be seen from Table 2 that the HBA capacity of the studied PB-RTILs, as measured by the β parameter is two times or more than the NB-RTILs and even, higher than water. This result is in agreement with a previous report of Breitbach & Armstrong [47], who have found that the HBA capacity of ILs is one of the most important interactions with the different analytes. This behavior was attributed to the basicity of the chloride anion. The high electron density and small size-to-charge ratio of this anion makes it an extremely strong hydrogen bond acceptor.

The HBD probe *4*-nitroaniline used to obtain the β parameter can only form hydrogen bonds with the anion of the PB-RTILs. If we compare $[(C_6)_3C_{14}P][Cl]$ and $[(C_6)_3C_{14}P][Br]$, (*c.f.* Fig. 1), their β values are higher than $[(C_6)_3C_{14}P][N(CN)_2]$ and $[(C_6)_3C_{14}P][NTf_2]$, which have bigger monovalent anions. The $N(CN)_2^-$ and NTf_2^- anions have much bigger size than Cl^- or Br^-, and the delocalization of their negative charge makes them weaker HBA and, as a consequence, the β values lower.

The β parameters for NB-RTILs are lower than the corresponding values for PB-RTILs and similar to those for ethyl acetate and acetonitrile (c.f. Table 2). A decreasing order of HBA capacity is as follows: $[OH–C_3NH_3][For]$, $[OH–C_2NH_3][For]$ > $[OMIM][BF_4]$, $[OMIM][PF_6]$, $[OPy][BF_4]$ > [HMIM][PF_6], and [BMIM][PF_6]. This trend can be explained by considering the HBA not only for the anion but also for the cation, if appropriate. Thus, the higher basicity for the $[OH–C_2NH_3][For]$ and $[OH–C_3NH_3][For]$ is due to both the HBA capacity of the formate anion and the hydroxyl group of the cation. For the $[OMIM][BF_4]$, $[OMIM][PF_6]$, and $[OPy][BF_4]$. the HBA capacity is due mainly to the anion, since the cations have the electron pairs of the N atoms compromised in the aromatic system. Finally, the lowest β values correspond to the [BMIM][PF_6] f [HMIM][PF_6]. Since the HBA capacity can be attributed only to the anion, the lower size-to-charge ratio of the PF_6^- anion makes this anion less basic. The BF_4^- anion has a smaller size-to-charge ratio than the PF_6^- anion [26,28]. Thus, the higher β value of the $[OMIM][PF_6]$ is unexpected.

3.1.3. α parameter

The HBD capacity for the studied RTILs could be arranged in three different families in decreasing order of α values: i. $[OH–C_2NH_3][For]$, $[OH–C_3NH_3][For]$ (near to $\alpha = 1$) which can be attributed to the –OH groups; ii. [BMIM][PF_6], [HMIM][PF_6], $[OMIM][BF_4]$, [OMIM][PF_6], $[OPy][BF_4]$, (α between 0.52 and 0.64) which can be attributed to the H atom attached to C2 of the imidazolium [28] and pyridinium rings. In the case of the imidazolium cation, the H atom is acidic in such a way that carbene formation is possible [48]. Recently, Skarmoutsos et al. [49] have provided a new insight about hydrogen-bonding in 1-butyl and 1-ethyl-methylimidazolium chloride. They concluded that the H atoms in α position to the N atoms impact significantly on H-bond networking, and a larger percentage of Cl^- anions coordinate to multiple cations via these first H atoms; iii. the PB-RTILs for which the HBD capacity is very low (α between 0.17 and 0.27, close to the α value for acetonitrile, see Table 2). Breitbach & Armstrong have used the SPM and obtained LSER coefficients for PB-RTILs showing that they are HBD solvents, i.e., **b** coefficient in Eq. 1 is different from 0. They considered this observation as "unrealistic" since it is against intuition. From a rapid evaluation of the chemical structures (c.f. Fig. 1), we could say that no acidic hydrogen atoms are present in the IL molecule. However, this apparently strange behavior could be explained if we take into account the acidity of the α-hydrogen atoms attached to the C–P bond ($–H_2C–P$). The acidity of this H atom is the base for the Wittig reaction [50] which leads to the formation of a carbene anion, –P(HC–)R, in the presence of a strong base such as $CO_3^=$.

3.1.4. E_T^N parameter

This solvatochromic parameter reflect both, polarity–polarizability and HBD capacity of the solvent, as expressed by Eq. 8. Since π^* values are quite similar for all the studied RTILs, the α values prevails in the behavior of the E_T^N parameter. Thus, the physicochemical interpretation of the obtained values are similar to the one given before for the α parameter. For 1-methyl-3-alkylimidazolium and pyridinium RTILs the E_T^N values are between 0.60 and 0.66 (close for ethanol, Table 2), in agreement with literature values (between 0.53–0.75 and 0.63–0.69, respectively) [42]. However, for the hydroxyalkylammonium RTILs the E_T^N values are higher than the previous ones and close to the pure water (Table 2).

For the PB-RTILs, polarity values increases from 0.39 to 0.44, which is also in agreement with literature values for tetraalkyl phosphonium salts, $[R_4P][X]$ (0.35–0.44). These values are equivalent to the polarity of acetone ($E_T^N = 0.355$) [42].

3.2. Application of the obtained solvent parameters in the chemical interpretation of partition phenomena

The obtained solvent parameters should be useful to explain and predict a given free-energy related property, such as equilibrium or kinetic constants, solubility and partition data. However, at present, there is no enough data in the literature about those physicochemical properties measured systematically in different RTILs. Thus, we will use the obtained solvent parameters obtained in this work to explain the LSER coefficients of Eq. 1 obtained in our previous studies of partition of analytes of very different chemical nature between RTILs and water [26,28].

As explained in Introduction, those LSER coefficients reflect the interactions between the solute and the biphasic system RTIL/water. Eq. 2 of the SPM shows that solute interacts with the IL phase and the water phase through polarity–polarizability ($\mathbf{s_{IL}}$ and $\mathbf{s_w}$), hydrogen bonding ($\mathbf{a_{IL}}$, $\mathbf{a_w}$, $\mathbf{b_{IL}}$ and $\mathbf{b_w}$), dispersive and cohesive interactions ($\mathbf{v_{IL}}$ and $\mathbf{v_w}$) and through electron-donor groups ($\mathbf{e_{IL}}$ and $\mathbf{e_w}$). Unfortunately, there is no solvent parameters accounting for dispersive interactions alone (**D** coefficients in Eq. 3), neither electron-donor groups. The $\boldsymbol{\sigma}$ coefficients in Eq. 3 can be represented by the Hildebrand solubility parameter, δ_H^2, but unfortunately it is available only for some RTILs. Thus, there is no data to explain the **e** coefficients and the experimental behavior for the **v** coefficients can be explained partially by the δ_H^2 values shown in Table 2. However, we could have a direct measurement of the **s**, **a** and **b** coefficients by using the obtained solvent parameters of Kamlet and Taft π^*, α and β respectively.

Eq. 1 has been previously used to both predict partitioning and to interpret the LSER coefficients and, thus, the chemical interactions present in the biphasic systems [BMIM][PF_6]/water and [HMIM][PF_6]/water [51]. In our previous works [26,28], we obtained partition coefficients, $P_{IL/w,}$ for several compounds, some of biological or pharmacological interest, between different RTILs (containing the imidazolium, pyridinium and phosphonium cations) and water at room temperature. We also used Eq. 1 to both predict partitioning and to interpret the LSER coefficients obtained. The LSER coefficients (or system constants) of Eq. 1 together with the standard deviation and coefficients of the determinations for the NB- and PB-RTILs studied in this work, as well as for the three previously reported NB-RTILs, are shown in Table 3. For both the NB-RTILs and the PB-RTILs, the two most influential intermolecular interactions affecting the partition process are the HBA capacity (β) of the solute (*negative* **b** term which accounts for the complementary property of the solvent, α) and the cavity-dispersion term (*positive* **v**

Table 3
LSER coefficients of Eq. 1 at 25 °C.

Ionic liquids	v	b	a	s	e
Anion: hexafluorophosphate, $[PF_6]^-$					
[BMIM][PF_6][a]	1.3 ± 0.3	−3.3 ± 0.1	−1.2 ± 0.1	−0.5 ± 0.1	1.0 ± 0.2
[HMIM][PF_6][a]	2.1 ± 0.3	−2.9 ± 0.2	−1.8 ± 0.1	−0.2 ± 0.1	1.4 ± 0.2
[OMIM][PF_6][b]	3.5 ± 0.3	−3.4 ± 0.2	−1.5 ± 0.1	−0.2 ± 0.1	1.0 ± 0.2
Anion: tetrafluoroborate, $[BF_4]^-$					
[OMIM][BF_4][a]	1.9 ± 0.3	−2.8 ± 0.2	−0.3 ± 0.2	−0.5 ± 0.2	1.2 ± 0.3
[OPy][BF_4][b]	2.5 ± 0.3	−2.7 ± 0.2	−0.3 ± 0.1	−0.7 ± 0.2	2.2 ± 0.4
Cation: trihexyl-(tetradecyl)phosphonium, $[(C_6)_3C_{14}P]^+$					
[$(C_6)_3C_{14}P$][Cl][b]	3.5 ± 0.4	−2.6 ± 0.2	1.5 ± 0.2	−1.1 ± 0.2	–
[$(C_6)_3C_{14}P$][Br][b]	3.6 ± 0.3	−3.5 ± 0.1	1.8 ± 0.1	−0.2 ± 0.1	–
[$(C_6)_3C_{14}P$][$N(CN)_2$][b]	3.5 ± 0.6	−5.3 ± 0.2	−0.4 ± 0.2	−0.8 ± 0.2	3.5 ± 0.4
[$(C_6)_3C_{14}P$][NTf_2][b]	2.7 ± 0.4	−3.5 ± 0.2	−1.5 ± 0.1	0.4 ± 0.1	–
[$(C_6)_3C_{14}P$][Cl][b]	3.5 ± 0.4	−2.6 ± 0.2	1.5 ± 0.2	−1.1 ± 0.2	–

Data from reference.
[a] [26].
[b] [28].

term). For the analysis shown below, it is important to remember that the LSER coefficients of Eq. 1 reflect the differences between the RTIL phase and aqueous phase in polarity–polarizability (**s** coefficient), HBA (**b** coefficient), HBD (**a** coefficient), cohesion–dispersion interactions (**v** coefficient) and polarizability interactions with electron-donor groups (**e** coefficient).

3.2.1. The *v* coefficient

The **v** coefficient: reflects the ability of the ionic liquid phase (IL) relative to the water phase (w) to interact through dispersive (**D**) and cohesive ($\boldsymbol{\sigma}$) interactions (Eq. 3). As can be observed in Table 3, the **v** coefficient is positive and large in all cases, which indicates that the RTILs are less cohesive and more polarizable than water.

For the three RTILs with the anion PF_6^-, the **v** coefficient increases with the alkyl chain of the cation. This could be attributed to the stronger dispersive interactions with the analyte as the alkyl chain increases and, simultaneously, to the decreasing of cohesivity, as reflected by the Hildebrand solubility parameter (*c.f.* Table 2). It can be observed that the **v** coefficient for [OPy][BF_4] is larger than for [OMIM][BF_4]. Since both have the same anion, this means that the cohesivity is lower for the OPy^+ cation as compared to the $OMIM^+$ or that the dispersive interactions are larger. This last observation is in agreement with the higher amount of carbon atoms of the OPy^+ cation.

Comparing the two NB-RTILs with the same cation, it can be seen from Table 3 that the **v** coefficient for [OMIM][BF_4] is lower than for [OMIM][PF_6]. From the solubility parameters in Table 2, that LSER coefficient should be higher for the latter RTIL, for which the δ_H^2 value is higher than for the [OMIM][BF_4]. However, dispersive interactions seem to be predominating in this case probably because the anion PF_6^- is more polarizable than the BF_4^-.

As can be seen from Table 3, similar or larger **v** coefficients for the PB-RTILs compared to NB-RTILs were obtained. The reason could be the stronger dispersive interactions that can be established with the four long alkyl chains present in PB-RTILs (*c.f.* Fig. 1). This observation is also in agreement with the lower δ_H^2 values for [$(C_6)_3C_{14}P$][Cl] and [$(C_6)_3C_{14}P$][NTf_2] as compared with the NB-RTILs.

3.2.2. The *b* coefficient ($\boldsymbol{a_{IL}}$–$\boldsymbol{a_w}$)

The **b** coefficient ($\mathbf{a_{IL}}$–$\mathbf{a_w}$): reflects the interactions between the solute as HBA and the medium as HBD. The **b** coefficient is negative and large in all cases, indicating that the RTIL phase is much less acidic than the water phase. This feature is in agreement with the Kamlet–Taft α parameter for these ILs, whose values are between 0.58 and 0.64 (*c.f.* Table 3) for the nitrogen-based RTILs and between 0.17–0.27 for the PB-RTILs. All these α values are lower than for water.

For the imidazolium-based RTILs the obtained α values match very well with the previously reported values [46,52]. As explained before, the HBD capacity of these RTILs can be attributed to the H atom attached to the C2 of the imidazolium ring (*c.f.* Fig. 1). For the PB-RTILs the observed HBD capacity can be related to the H atoms in the α position to the P atom, as discussed in Section 3b for α parameter.

3.2.3. The *a* coefficient ($\boldsymbol{b_{IL}}$–$\boldsymbol{b_w}$)

The **a** coefficient ($\mathbf{b_{IL}}$–$\mathbf{b_w}$): reflects the interactions between the solute as HBD and the medium as HBA. These LSER coefficients are negative for all NB-RTILs meaning that the ionic liquid phase has less HBA capacity compared to water. This result is consistent with the lower β values for these RTILs as compared to water (*c.f.* Table 3). The studied NB-cations cannot accept a hydrogen bond since the N atoms have no free electron pairs. Thus, the anions are responsible for the observed HBA capacity.

For the NB-RTILs containing the PF_6^- anion, the **a** coefficient is large as compared to those containing the BF_4^- anion. Since **a** coefficient is negative, this means that the HBA capacity for those RTILs is lower than the RTILs containing the BF_4^- anion, which is supported by the experimental β values in Table 3. The higher electron density of the BF_4^- anion compared to the PF_6^- anion could explain this behavior.

As occurs for the NB-RTILs, for the PB-RTILs the corresponding cations cannot accept a hydrogen bond neither. Thus, HBA capacity is also attributed only to the anion. According to the high β values shown in Table 3, the **a** coefficients should always be positive since β_{IL} is higher than β_w and, thus, $\mathbf{b_{IL}}$ should always be higher than $\mathbf{b_w}$. The **a** coefficient is positive and large for [$(C_6)_3C_{14}P$][Cl] and [$(C_6)_3C_{14}P$][Br]. This behavior can be explained by the high HBA capacity of the Cl^- and Br^- anions because of its high electron density.

However, the **a** coefficient is negative for [$(C_6)_3C_{14}P$][$N(CN)_2$] and [$(C_6)_3C_{14}P$][NTf_2]. The β values of Table 2 for these RTILs are smaller than for [$(C_6)_3C_{14}P$][Cl] and [$(C_6)_3C_{14}P$][Br]. This result could be attributed to the much bigger size of the $N(CN)_2^-$ and NTf_2^- anions which make them much weaker HBA. The negative **a** values for these two RTILs could be attributed to the mutual solubility RTIL-water. According to the β parameters for the neat solvents, the presence of the ionic liquid in water *increases* its HBA capacity (and thus, the $\mathbf{b_w}$ term) while the presence of water in the ionic liquid phase *decreases* its HBA capacity (and thus, the $\mathbf{b_{IL}}$ term). As a consequence, a negative **a** coefficient can be possible, depending on the mutual solubility IL/water.

Since the **a** coefficient reflects the HBA capacity, a comparison of the different anions can be made independently of the RTIL type. Thus, an arrangement from the weakest to the strongest HBA (smaller to the larger $\mathbf{b_{IL}}$ term) can be made for the studied RTILs: PF_6^-, NTf_2^- < BF_4^-, $N(CN)_2^-$ < Cl^-, Br^-. Since all anions have the same charge, this order is

parallel to the decreasing size, i.e., chloride and bromide anions have the strongest HBA capacity which makes the $\mathbf{b_{IL}}$ term larger and, thus, the **a** coefficient lower than for the other anions. In general, the β values of Table 2 follow very well the $\mathbf{b_{IL}}$ term values that can be obtained from the obtained **a** coefficient.

3.2.4. The *s* coefficient (s_{IL}–s_w)

The **s** coefficient ($\mathbf{s_{IL}}$–$\mathbf{s_w}$): reflects the polarity-polarizability interactions between the biphasic system and the solute. Except for $[(C_6)_3C_{14}P][NTf_2]$, the **s** coefficient is quite small and negative, indicating that the polarity of the RTIL phase is a little smaller than the polarity of the aqueous phase. This observation is in agreement with previous results for other RTILs [8] and it is supported by their respective polarity–polarizability parameters π^* shown in Table 2. Due to the ionic character of the RTILs, a higher polarity could be expected as compared to water. This fact was only observed for $[(C_6)_3C_{14}P][NTf_2]$. Again, this apparent anomaly could be attributed, at least in part, to the mutual solubility RTIL-water.

3.2.5. The *e* coefficient

The **e** coefficient: reflects the polarizability interactions between the medium and the solute through π and nonbonding electrons and it can be written as $\mathbf{e_{IL}}$–$\mathbf{e_w}$ [26]. The **e** coefficient of Table 3 is quite high and positive for the NB-RTILs and for $[(C_6)_3C_{14}P][N(CN)_2]$, indicating that the polarizability is higher for the RTIL phase than for the water phase. For the NB-RTILs, the **e** coefficients reflect the polarizability due to the π electrons of the cations while, for the $[(C_6)_3C_{14}P][N(CN)_2]$ it reflects the polarizability due to the π electrons of the anion (no free electron pairs neither π electrons are present in any phosphonium cation).

Thus, it is possible to conclude that the obtained solvatochromic parameter of Kamlet and Taft are helpful to explain the LSER coefficients obtained through the Solvation Parameter Model for partition data. However, some conclusions should be drawn with care since the obtained π, α and β parameters for neat solvents could not reflect the actual **s**, **a**, **b** values because of the mutual solubility water/RTILs.

4. Conclusions

Solvatochromic solvent parameters E_T^N(polarity–polarizability and hydrogen-bond acidity), π^* (polarity–polarizability), α (hydrogen-bond acidity) and β (hydrogen-bond basicity) for different nitrogen-based and phosphonium-based room-temperature ionic liquids were accurately determined. The obtained parameters were in quite well in agreement with the chemical structure of the respective RTILs and were useful to explain the physicochemical meaning of the regression coefficients obtained with the Solvation Parameter Model applied to partition data in different RTIL/water systems.

Acknowledgments

Financial support from the Consejo Nacional de Investigaciones Científicas y Técnicas (CONICET) (PIP 0244) and Agencia Nacional de Promoción Científica y Técnica (ANPCYT 2014-3597) is gratefully acknowledged. M. Reta is a scientific member of CONICET and Professor of Analytical Chemistry at the Universidad Nacional de La Plata (Argentina). J.M. Padró is a research fellow of CONICET. The authors want to thank to all of these scientific organizations.

References

[1] P. Wasserscheid, T. Welton, Ionic Liquid in Synthesis, Wiley-VCH Verlag GmbH & Co., Weinheim, Germany, 2002.
[2] T. Welton, Room-temperature ionic liquids. Solvents for synthesis and catalysis, Chem. Rev. 99 (1999) 2071–2084.
[3] C.M. Gordon, New developments in catalysis using ionic liquids, Appl. Catal. A Gen. 222 (2001) 101–117.
[4] R.A. Sheldon, R.M. Lau, M.J. Sorgedrager, F. van Rantwijk, K.R. Seddon, Biocatalysis in ionic liquids, Green Chem. 4 (2002) 147–151.
[5] T. Kakiuchi, N. Nishi, Ionic liquid|water interface: a new electrified system for electrochemistry, Electrochemistry 74 (2006) 942–948.
[6] T. Sato, G. Masuda, K. Takagi, Electrochemical properties of novel ionic liquids for electric double layer capacitor applications, Electrochim. Acta 49 (2004) 3603–3611.
[7] A.E. Visser, R.P. Swatloski, R.D. Rogers, pH-Dependent partitioning in room temperature ionic liquids provides a link to traditional solvent extraction behavior, Green Chem. 2 (2000) 1–4.
[8] C.F. Poole, S.K. Poole, Extraction of organic compounds with room temperature ionic liquids, J. Chromatogr. A. 1217 (2010) 2268–2286.
[9] L.B. Escudero, A. Castro Grijalba, E.M. Martinis, R.G. Wuilloud, Bioanalytical separation and preconcentration using ionic liquids, Anal. Bioanal. Chem. 405 (2013) 1–17.
[10] E.M. Martinis, P. Berton, R.P. Monasterio, R.G. Wuilloud, Emerging ionic liquid-based techniques for total-metal and metal-speciation analysis, TrAC Trends Anal. Chem. 29 (2010) 1184–1201.
[11] C.F. Poole, Chromatographic and spectroscopic methods for the determination of solvent properties of room temperature ionic liquids, J. Chromatogr. A. 1037 (2004) 49–82.
[12] S. Pandey, Analytical applications of room-temperature ionic liquids: a review of recent efforts, Anal. Chim. Acta 556 (2006) 38–45.
[13] W.E. Acree, L.M. Grubbs, Anal. Appl. of Ion. Liq. (2012)http://dx.doi.org/10.1002/9780470027318.a9153.
[14] P. Sun, D.W. Armstrong, Ionic liquids in analytical chemistry, Anal. Chim. Acta 661 (2010) 1–16.
[15] J.G. Huddleston, A.E. Visser, W.M. Reichert, H.D. Willauer, G.A. Broker, R.D. Rogers, Characterization and comparison of hydrophilic and hydrophobic room temperature ionic liquids incorporating the imidazolium cation, Green Chem. 3 (2001) 156–164.
[16] D. Zhao, J. Wang, E. Zhou, Oxidative desulfurization of diesel fuel using a Bronsted acid room temperature ionic liquid in the presence of H2O2, Green Chem. 9 (2007) 1219–1222.
[17] C. Reichardt, Polarity of ionic liquids determined empirically by means of solvatochromic pyridinium N-phenolate betaine dyes, Green Chem. 7 (2005) 339–351.
[18] V.G. Machado, R.I. Stock, C. Reichardt, Pyridinium N-Phenolate Betaine Dyes 114 (2014) 10429–10475.
[19] P.G. Jessop, D.A. Jessop, D. Fu, L. Phan, Solvatochromic parameters for solvents of interest in green chemistry, Green Chem. 14 (2012) 1245–1259.
[20] N.D. Khupse, A. Kumar, Contrasting thermosolvatochromic trends in pyridinium-, pyrrolidinium-, and phosphonium-based ionic liquids, J. Phys. Chem. B. 114 (2010) 376–381.
[21] M.A. Ab Rani, A. Brant, L. Crowhurst, A. Dolan, M. Lui, N.H. Hassan, et al., Understanding the polarity of ionic liquids, Phys. Chem. Chem. Phys. 13 (2011) 16831–16840.
[22] L. Crowhurst, R. Falcone, N.L. Lancaster, V. Llopis-Mestre, T. Welton, Using Kamlet–Taft solvent descriptors to explain the reactivity of anionic nucleophiles in ionic liquids, J. Org. Chem. 71 (2006) 8847–8853.
[23] B.R. Mellein, S.N.V.K. Aki, R.L. Ladewski, J.F. Brennecke, Solvatochromic studies of ionic liquid/organic mixtures, J. Phys. Chem. B. 111 (2006) 131–138.
[24] J.-M. Lee, S. Ruckes, J.M. Prausnitz, Solvent polarities and Kamlet–Taft parameters for ionic liquids containing a pyridinium cation, J. Phys. Chem. B. 112 (2008) 1473–1476.
[25] A. Sarkar, S. Trivedi, G.A. Baker, S. Pandey, Multiprobe spectroscopic evidence for "hyperpolarity" within 1-butyl-3-methylimidazolium hexafluorophosphate mixtures with tetraethylene glycol, J. Phys. Chem. B. 112 (2008) 14927–14936.
[26] J.M. Padró, A. Ponzinibbio, L.B. Agudelo Mesa, M. Reta, Predicting the partitioning of biological compounds between room-temperature ionic liquids and water by means of the solvation-parameter model, Anal. Bioanal. Chem. 399 (2011) 2807–2820.
[27] K.J. Fraser, D.R. MacFarlane, Phosphonium-based ionic liquids: an overview, Aust. J. Chem. 62 (2009) 309–321.
[28] J.M. Padró, R.B. Pellegrino Vidal, M. Reta, Partition coefficients of organic compounds between water and imidazolium-, pyridinium-, and phosphonium-based ionic liquids, Anal. Bioanal. Chem. 406 (2014) 8021–8031.
[29] M. Reta, P.W. Carr, P.C. Sadek, S.C. Rutan, Comparative study of hydrocarbon, fluorocarbon, and aromatic bonded RP-HPLC stationary phases by linear solvation energy relationships, Anal. Chem. 71 (1999) 3484–3496.
[30] J. Gotta, S. Keunchkarian, C. Castells, M. Reta, Predicting retention in reverse-phase liquid chromatography at different mobile phase compositions and temperatures by using the solvation parameter model, J. Sep. Sci. 35 (2012) 2699–2709.
[31] M.H. Abraham, A. Ibrahim, A.M. Zissimos, Determination of sets of solute descriptors from chromatographic measurements, J. Chromatogr. A. 1037 (2004) 29–47.
[32] I. Cacelli, S. Campanile, A. Giolitti, D. Molin, Theoretical prediction of the Abraham hydrogen bond acidity and basicity factors from a reaction field method, J. Chem. Inf. Model. 45 (2005) 327–333, http://dx.doi.org/10.1021/ci049688f.
[33] J. Li, Y. Zhang, H. Ouyang, P.W. Carr, Gas chromatographic study of solute hydrogen bond basicity, J. Am. Chem. Soc. 114 (1992) 9813–9828.
[34] M.J. Kamlet, M.H. Abraham, P.W. Carr, R.M. Doherty, R.W. Taft, Solute-solvent interactions in chemistry and biology. Part 7. An analysis of mobile phase effects on high pressure liquid chromatography capacity factors and relationships of the latter with octanol-water partition coefficients, J. Chem. Soc. Perkin Trans. 2 (1988) 2087–2092.
[35] A. Marciniak, The solubility parameters of ionic liquids, Int. J. Mol. Sci. 11 (2010) 1973–1990.
[36] J.M. Padró, Coeficientes de Partición Entre Líquidos Iónicos y Agua, Aplicación a la microextracción dispersiva de compuestos antichagásicos en muestras biológicas, UNLP, 2014.

[37] D. Fang, K. Gong, Q.-R.Q.-R. Shi, X.-L.X.-L. Zhou, Z.-L.Z.-L. Liu, J. Cheng, A green and novel procedure for the preparation of ionic liquid, J. Fluor. Chem. 129 (2008) 108–111.
[38] N. Bicak, A new ionic liquid: 2-hydroxy ethylammonium formate, J. Mol. Liq. 116 (2005) 15–18.
[39] M. Reta, R. Cattana, J.J. Silber, Kamlet–Taft's solvatochromic parameters for nonaqueous binary mixtures between n-hexane and 2-propanol, tetrahydrofurane, and ethyl acetate, J. Solut. Chem. 30 (2001) 237–252.
[40] C. Reichardt, Solvent and Solvent Effects in Organic Chemistry, VCH Verlagsgesellshaft mbH, Weinheim, Germany, 1988.
[41] M.J. Muldoon, C.M. Gordon, I.R. Dunkin, Investigations of solvent–solute interactions in room temperature ionic liquids using solvatochromic dyes, J. Chem. Soc. Perkin Trans. 2. (2001) 433–435.
[42] S. Coleman, R. Byrne, S. Minkovska, D. Diamond, Thermal reversion of spirooxazine in ionic liquids containing the [NTf 2]- anion, Phys. Chem. Chem. Phys. 11 (2009) 5608–5614.
[43] M.J. Kamlet, J.L. Abboud, R.W. Taft, The solvatochromic comparison method. 6. The π scale of solvent polarities, J. Am. Chem. Soc. 99 (1977) 8325–8327.
[44] Y. Migron, Y. Marcus, Polarity and hydrogen-bonding ability of some binary aqueous-organic mixtures, J. Chem. Soc. Faraday Trans. 87 (1991) 1339–1343.
[45] Y. Marcus, The properties of organic liquids that are relevant to their use as solvating solvents, Chem. Soc. Rev. 22 (1993) 409–416.
[46] L. Crowhurst, P.R. Mawdsley, J.M. Perez-Arlandis, P.A. Salter, T. Welton, Solvent–solute interactions in ionic liquids, Phys. Chem. Chem. Phys. 5 (2003) 2790–2794.
[47] D.W. Armstrong, Z.S. Breitbach, Characterization of phosphonium ionic liquids through a linear solvation energy relationship and their use as GLC stationary phases, Anal. Bioanal. Chem. 390 (2008) 1605–1617.
[48] S. Chowdhury, R.S. Mohan, J.L. Scott, Reactivity of ionic liquids, Tetrahedron 63 (2007) 2363–2389.
[49] I. Skarmoutsos, D. Dellis, R.P. Matthews, T. Welton, P.A. Hunt, Hydrogen bonding in 1-butyl- and 1-ethyl-3-methylimidazolium chloride ionic liquids, J. Phys. Chem. B. 116 (2012) 4921–4933.
[50] Y. Moussaoui, K. Saïd, R.B. Salem, Anionic activation of the Wittig reaction using a solid–liquid phase transfer: examination of the medium-, temperature-, base- and phase-transfer catalyst effects, ARKIVOC 2006 (2006) 1–22.
[51] M.H. Abraham, A.M. Zissimos, J.G. Huddleston, H.D. Willauer, R.D. Rogers, W.E. Acree, Some novel liquid partitioning systems: water–ionic liquids and aqueous biphasic systems, Ind. Eng. Chem. Res. 42 (2003) 413–418.
[52] S.N. Baker, G.A. Baker, F.V. Bright, Temperature-dependent microscopic solvent properties of "dry" and "wet" 1-butyl-3-methylimidazolium hexafluorophosphate: correlation with ET(30) and Kamlet–Taft polarity scales, Green Chem. 4 (2002) 165–169.
[53] A. Jeličić, N. García, H.-G. Löhmannsröben, S. Beuermann, Prediction of the ionic liquid influence on propagation rate coefficients in methyl methacrylate radical polymerizations based on Kamlet–Taft solvatochromic parameters, Macromolecules 42 (2009) 8801–8808.
[54] H. Salari, M. Khodadadi-Moghaddam, A.R. Harifi-Mood, M.R. Gholami, Preferential solvation and behavior of solvatochromic indicators in mixtures of an ionic liquid with some molecular solvents, J. Phys. Chem. B. 114 (2010) 9586–9593.
[55] S. Zhang, Z. Chen, X. Qi, Y. Deng, Distinct influence of the anion and ether group on the polarity of ammonium and imidazolium ionic liquids, New J. Chem. 36 (2012) 1043–1050.
[56] R. Lungwitz, V. Strehmel, S. Spange, The dipolarity/polarisability of 1-alkyl-3-methylimidazolium ionic liquids as function of anion structure and the alkyl chain length, New J. Chem. 34 (2010) 1135–1140.
[57] P.K. Kilaru, P. Scovazzo, Correlations of low-pressure carbon dioxide and hydrocarbon solubilities in imidazolium-, phosphonium-, and ammonium-based room-temperature ionic liquids. Part 2. Using activation energy of viscosity, Ind. Eng. Chem. Res. 47 (2007) 910–919.